Cost-Benefit Assessment of Climate and Weather Optimized Trajectories for Different North Atlantic Weather Patterns

Lührs, Benjamin; Niklaß, Malte ; Frömming, Christine; Grewe, Volker; Gollnick, Volker

Publication date
2018

Document Version
Final published version

Published in
Proceedings of the 31st Congress of the International Council of the Aeronautical Sciences

31st Congress of the International Council of the Aeronautical Sciences

Belo Horizonte, Brazil; September 09-14, 2018

COST-BENEFIT ASSESSMENT OF CLIMATE AND WEATHER OPTIMIZED TRAJECTORIES FOR DIFFERENT NORTH ATLANTIC WEATHER PATTERNS

Benjamin Lührs[1], Malte Niklaß[2], Christine Frömming[3], Volker Grewe[3,4], Volker Gollnick[1,2]

[1]Technische Universität Hamburg (TUHH), Institut für Lufttransportsysteme,
[2]Deutsches Zentrum für Luft und Raumfahrt (DLR), Lufttransportsysteme,
[3]Deutsches Zentrum für Luft und Raumfahrt (DLR), Institut für Physik der Atmosphäre,
[4]Delft University of Technology (TU Delft), Section Aircraft Noise & Climate Effects

Keywords: *Climate impact mitigation – Non-CO_2 emissions – Trajectory optimization Optimal control – Cost-benefit analysis*

Abstract

Besides CO_2, the climate impact of commercial aviation is strongly influenced by non-CO_2 effects, which are highly sensitive to meteorological conditions and their spatial variations. To assess the cost-benefit potential (climate impact mitigation vs. cost increase) of climate and weather optimized flight trajectories in the North Atlantic flight corridor, optimal control techniques are applied. However, the execution of multi-criteria route optimizations for an intercontinental route network and various weather patterns is computationally highly intensive. Since computational resources are limited, a reduced surrogate route network is generated and evaluated first with regard to the computational effort, the coverage in terms of available seat kilometers, as well as the accuracy of reproducing the original route network with regard to climate impact. The proposed reduced route network consists of 40 routes (original network: 1,359) and is able to reproduce the climate impact of the original route network with reasonable climate impact deviations of 2.5%.
The evaluation of climate and weather optimized trajectories is performed for the top route of the surrogate network. The maximum climate impact reduction potential is differing strongly from 9% up to 60% for varying North Atlantic weather patterns. Averaged over the weather patterns, a maximum climate impact mitigation potential of about 32%, going along with a cost increase of about 8% has been estimated. However, at a cost penalty of 1%, a potential climate impact reduction of 24% has been observed.

1 Introduction

Impacts of commercial aviation upon the climate are expected to increase since predicted growth rates in terms of passenger kilometers (4-5% per year) [1] highly surpass annual fuel efficiency improvements of about 1-2% [2]. A significant part of aviation's climate impact arises from non-CO_2 effects, e.g. changes in the atmospheric composition of ozone and methane as well as contrail induced cloudiness (CiC). Since non-CO_2 effects are highly sensitive to meteorological conditions, there are further interdependencies between aircraft emissions and climate impact apart from the amount of emitted climate agents, as in case of CO_2 [3]. Hence, there is a high spatial and temporal dependency of non-CO_2 climate effects which makes the associated climate impact estimations much more difficult but offers the possibility of climate impact mitigation by re-routing.
Most reliable climate impact assessments can therefore be obtained only with detailed chemistry-climate and general circulation model simulations, which are very computationally intensive limiting the number of feasible analyses. To reduce the computational effort, simplified climate-response models are often used, which reproduce results of detailed chemistry-climate model simulations without calculating all complex processes. Once they are determined, e.g. five-dimensional climate

change functions[1] (CCFs), estimate the climate change contribution due to aircraft emissions as function of emission location, time and species with only low computational effort [4][5].
However, to approximate the Pareto front (climate impact mitigation vs. cost increase) of various mitigation options for a single route and a specific weather pattern, there is still a large number of trajectory simulations necessary. The computational effort increases quickly with an increasing number of routes and weather patterns. Since computational resources are limited, the question arises how to simplify a complex route network for the adequate assessment of different climate impact mitigation options without significantly affecting the evaluation accuracy.
In the following, modeling approaches for the assessment of climate impact mitigation options are described (see section 2). Furthermore, the original route network is introduced, and the surrogate network is described and evaluated (see section 3). Subsequently, cost-benefit analyses of climate and weather optimized trajectories are performed exemplarily for the top surrogate route and eight different North Atlantic weather patterns (see section 4). Finally, conclusions and future work are described (see section 5).

2 Modeling approach

For the estimation of continuously optimized aircraft trajectories, the *Trajectory Optimization Module* (TOM) is utilized which is based on an optimal control approach [6]. Consequently, aircraft's motion is described as temporal evolution of state variables $\boldsymbol{x}(t)$ and control variables $\boldsymbol{u}(t)$.
Optimized trajectories are determined by identifying a control input $\boldsymbol{u}(t)$ which minimizes the cost functional J according to Eq. (1). At the same time, dynamic constraints (e.g. equations of motion) as well as control (e.g. thrust limitations), state (e.g. maximum speed) and path limitations (e.g. maximum pressure altitude) have to be satisfied.

$$J(\boldsymbol{x}(t),\boldsymbol{u}(t),t) = c_\Psi \cdot \int_{t_0}^{t_f} \Psi(\boldsymbol{x}(t),\boldsymbol{u}(t),t)\,\mathrm{d}t + c_\Upsilon \cdot \Upsilon(t_0,t_f,\boldsymbol{x}(t_0),\boldsymbol{x}(t_f)) \tag{1}$$

$$c_\Psi + c_\Upsilon = 1 \quad \text{with} \quad c_\Psi, c_\Upsilon \in [0,1] \tag{2}$$

Generally, the cost functional J consists of a penalty function Υ which is a function of initial and final time t_0 and t_f as well as initial and final state $\boldsymbol{x}(t_0)$ and $\boldsymbol{x}(t_f)$. Moreover, J contains the temporal integral over a second penalty function $\Psi(\boldsymbol{x}(t),\boldsymbol{u}(t),t)$. The magnitudes of both penalty functions can be scaled with the corresponding weighting factors c_Ψ and c_Υ according to Eq. (2). Within this study, two different cost functionals are applied for calculating Pareto-optimal trajectories with regard to climate impact and economic aspects (see section 2.1) as well as orthodromes (see section 2.2).
The aircraft performance characteristics are obtained from Eurocontrol's base of aircraft data (BADA) 4.2 performance models [7]. Additionally, the aircraft emissions which are required for the climate impact evaluation, are estimated based on the Eurocontrol modified Boeing Fuel Flow Method 2 [8][9].
Using the MATLAB toolbox *GPOPS-II* [10], the resulting continuous optimal control problem is transformed into a discrete non-linear programming problem (NLP) which is then solved with the NLP-solver *IPOPT* [11].

2.1 Calculation of Pareto-optimal trajectories

To calculate trajectories which are Pareto-optimal with regard to climate impact and economic aspects, climate change functions (CCF, see section 2.1.1) and direct operating costs (DOC, see section 2.1.2) are integrated into the cost functional J.

$$J_{\text{Pareto}} = c_\Psi \cdot \left\{ \sum_i \int_{t_0}^{t_f} \mathrm{CCF}_i(\boldsymbol{x},t) \cdot \dot{m}_i(t)\,\mathrm{d}t + \cdots + \int_{t_0}^{t_f} \mathrm{CCF}_{\mathrm{CIC}}(\boldsymbol{x},t) \cdot v_{\mathrm{TAS}}(t)\,\mathrm{d}t \right\} \cdot \mathrm{ATR}_{20,\mathrm{ref}}^{-1} + \cdots + c_\Upsilon \cdot \left[\mathrm{DOC}\left(t_f - t_0, m_0 - m_f\right)\right] \cdot \mathrm{DOC}_{\mathrm{ref}}^{-1} \tag{3}$$

[1] CCFs form the basis for the simulation of climate and weather optimized flight trajectories and are computed individually for various weather patterns [4][5][6].

According to Eq. (3), the cost functional J is defined as the weighted sum of climate impact (curly brackets) and direct operating costs (squared brackets). Both values are normalized with respect to the corresponding values of the minimum DOC trajectory which is serving as reference. Pareto-optimal trajectories are obtained by varying the weights (c_Ψ, c_Υ) of climate impact and DOC: minimum climate impact trajectories are obtained for $c_\Psi = 1$ and minimum DOC trajectories for $c_\Upsilon = 1$.

2.1.1 Climate change functions

Climate change functions (CCFs) allow for the quantification of the climate impact caused by aircraft emissions as a function of emission location and time. Within this study, CCF($\boldsymbol{x}$,t) derived by Frömming et al. (2013) [4] are used which are based on simulations performed with the ECHAM5/MESSY Atmospheric Chemistry Model (EMAC) [12] for eight typical weather patterns in the North Atlantic region as classified by Irvine et al. (2013) [13]. The CCFs are serving as a measure for climate change and are calculated as average temperature response integrated over a time period of 20 years (ATR_{20}) individually for CO_2, H_2O and NO_x (ATR_{20} per unit emission) as well as contrail induced cloudiness (CiC, ATR_{20} per flown unit distance).[2] The coverage area of the CCFs is illustrated in Fig. 1 (solid red line).

2.1.2 Direct operating costs

DOC are computed by employing the TU Berlin DOC method as proposed by Thorbeck (2012) [14]. Here, route dependent costs – including the costs for fuel, crew, maintenance as well as landing, navigation and ground handling fees – are calculated as function of mission time ($t_f - t_0$), mission fuel ($m_0 - m_f$) and aircraft size (e.g. maximum take-off mass, payload). Additionally, capital costs – covering the costs for depreciation, interest and insurance – are primarily based on the size of the aircraft and its respective operational empty weight. For the fuel price, the average value of the year 2016 is assumed. All other costs are scaled to the year 2016 considering the US inflation rate of average consumer prices [15].

2.2 Calculation of orthodromes

Orthodromes serve as reference trajectories and ensure the comparability of the results. To minimize the flight distance over ground (s_{Ground}) TOM's cost functional J is defined as:

$$J_{\text{Orth}} = s_{\text{Ground}}(t_f) \qquad (4)$$

3 North Atlantic route network

Within this study, potential climate impact savings are estimated based on the scheduled North Atlantic civil air traffic for the year 2016. However, since computational resources are limited, the original route network (see section 3.1) was replaced with a reduced surrogate route network (see section 3.2).

3.1 Original North Atlantic route network

Using the worldwide Airport Data Intelligence (ADI) dataset of scheduled flights for the year 2016 [16], the original North Atlantic route network has been generated by applying multiple filters to the full dataset:

(1) only routes operated with Airbus (A310, A330, A340, A380) and Boeing (747, 757, 767, 777, 787) long-range aircraft are considered,
(2) the orthodrome between origin and destination of each route has to intersect the mean longitude line within the CCF coverage area (see red dashed line in Fig. 1),
(3) the maximum latitude of the orthodrome is below the northern bound of the CCF coverage area.

The resulting route network is illustrated in Fig. 1 and consists of 1,359 routes representing approximately 10.5 % of the available seat kilometers (ASK) worldwide.

[2] However, within this study, CiC has not been considered since an updated version of the corresponding CCFs is currently under development.

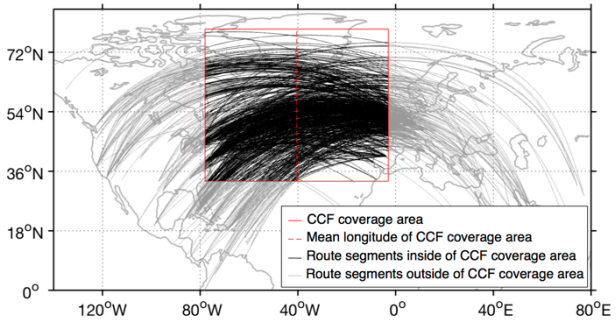

Fig. 1: Original North Atlantic route network.

All trajectory simulations are performed with an average load factor of 80.4 % which represents the adjusted ASK[3] weighted mean load factor of the original North Atlantic route network (see Fig. 2).

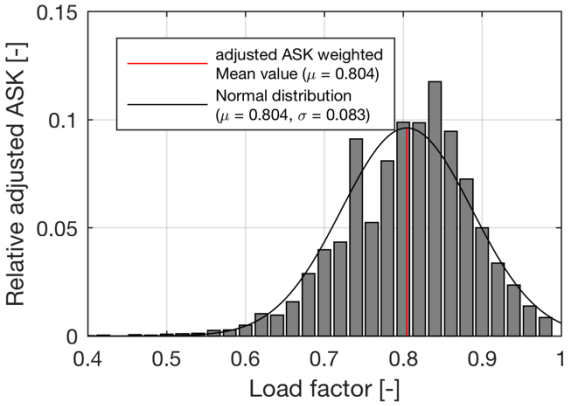

Fig. 2: Load factor distribution for the original North Atlantic route network.

3.2 Surrogate North Atlantic route network

Based on the previously described original North Atlantic route network for the year 2016, the generation of a reduced North Atlantic route network is explained in the following (see section 3.2.1). Subsequently, the ability of the reduced North Atlantic route network to serve as surrogate network for the original North Atlantic Route network is examined and evaluated against potential savings in terms of computational effort (see section 3.2.2).

3.2.1 Route network generation

The climate change functions (see section 2.1.1) as well as the associated weather conditions (e.g. wind, pressure, temperature) are only available within the CCF coverage area. For this reason, the reduced North Atlantic route network is constructed as network in between the edges of the CCF coverage area (see Fig. 3).

To generate a reduced route network, the western and eastern bounds of the CCF coverage area are divided into n equally spaced segments each with $\Delta\varphi = (\varphi_{\max} - \varphi_{\min})/n$ (see Fig. 3, segments A to G and a to g). Additionally, the southern bound is divided into segments of the same geometric length leading to $\Delta\lambda = \Delta\varphi/\cos(\varphi_{\min})$ for both, the western (H to L) and the eastern half (h to l).

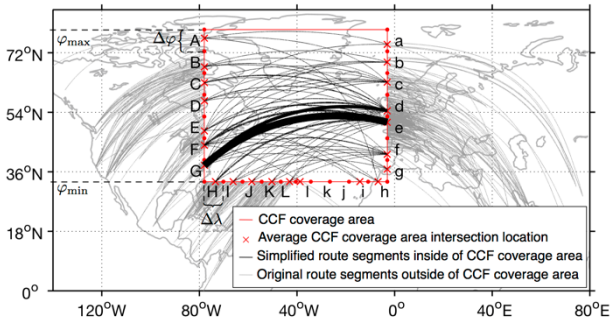

Fig. 3: Reduced North Atlantic route network for $n = 7$. The line thickness of the route segments is proportional to the cumulative adjusted ASK on this segment.

Subsequently, for all original routes, the intersection locations $(\lambda_x \mid \varphi_x)$ of the corresponding orthodrome with the CCF coverage area are determined and the original route is assigned to a surrogate route r from one western segment (A to L) to one eastern segment (a to l) or vice versa. As illustrated in Eq. (5) and (6), for each segment $s \in [A, B, \dots, a, b, \dots]$, the adjusted ASK weighted average intersection locations $\bar{\lambda}_s$ and $\bar{\varphi}_s$ are determined (see Fig. 3, red crosses). Here, n_s represents the number of original routes intersecting segment s.

$$\bar{\lambda}_s = \frac{\sum_{j=1}^{n_s} \lambda_{x,s,j} \cdot \mathrm{ASK}_{\mathrm{adj},s,j}}{\sum_{j=1}^{n_s} \mathrm{ASK}_{\mathrm{adj},s,j}} \tag{5}$$

$$\bar{\varphi}_s = \frac{\sum_{j=1}^{n_s} \varphi_{x,s,j} \cdot \mathrm{ASK}_{\mathrm{adj},s,j}}{\sum_{j=1}^{n_s} \mathrm{ASK}_{\mathrm{adj},s,j}} \tag{6}$$

For each surrogate route r from segment to segment, the cumulative adjusted ASK is

[3] The adjusted ASK for each route is defined as the ASK within the CCF coverage area (see Fig. 1).

determined according to Eq. (7), where n_r denotes the number of original routes being assigned to the surrogate route r.

$$\mathrm{ASK}_{\mathrm{adj},r} = \sum_{k=1}^{n_r} \mathrm{ASK}_{\mathrm{adj},r,k} \qquad (7)$$

In the next step, the most prominent aircraft type in terms of adjusted ASK is selected as representative aircraft type AC_r individually for each surrogate route r. Finally, the annual frequency f_r of route r of the surrogate network is calculated according to Eq. (8),

$$f_r = \frac{\mathrm{ASK}_{\mathrm{adj},r}}{d_r \cdot n_{\mathrm{Seats},\mathrm{AC}_r}} \qquad (8)$$

where d_r represents the orthodrome distance of route r and $\boldsymbol{n_{\mathrm{Seats},\mathrm{AC}_r}}$ the number of seats in the representative aircraft type AC_r. Exemplary results for $n = 7$ are shown in Tab. 1.

Tab. 1: Top 4 routes (adjusted ASK) of the surrogate route network for $n = 7$.

r	$\mathrm{ASK}_{\mathrm{adj},r,\mathrm{rel}}$	s_{Orgn}	s_{Dest}	f_r	AC_r
1	0.1359	e	G	42,482	777-300ER
2	0.1357	G	e	42,446	777-300ER
3	0.0640	d	G	20,363	777-300ER
4	0.0629	G	d	23,658	A330-300

3.2.2 Route network selection

To identify an appropriate fineness n of the surrogate route network, a tradeoff between the resulting computational effort, the ASK coverage as well as the accuracy of reproducing the original route network in terms of climate impact is required.

Fig. 4 shows the cumulative relative adjusted ASK as a function of the number of considered routes for route network fractions $n = 6 \ldots 10$. Here, the considered routes have been reordered, such that routes representing highest adjusted ASK are taken into account first. For a given number of considered routes, representing an estimate of the resulting computational effort, the coverage of adjusted ASK is a function of the route network fraction n: the lower the network fraction n, the higher the adjusted ASK coverage. If, for example, the simulation of 20 routes is accepted, 82% of the adjusted ASK can be covered for $n = 6$. In contrast, only 66% of the adjusted ASK are considered for $n = 10$. However small network fractions, are expected to result in a reduced accuracy in terms of climate impact.

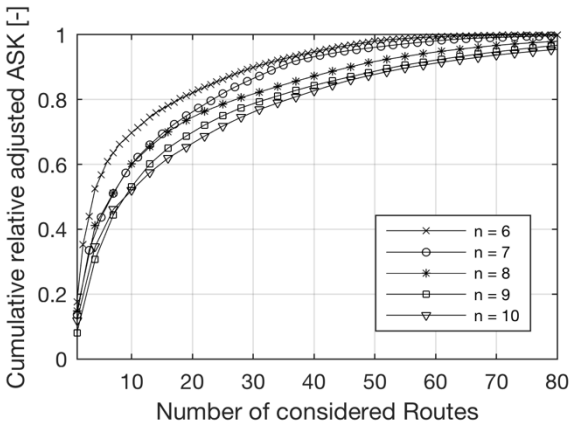

Fig. 4: Cumulative relative adjusted ASK as a function of the number of considered routes for different network fractions n.

To evaluate the accuracy in terms of the resulting climate impact, trajectory calculations are performed with TOM for both, the original as well as the surrogate route network within the CCF coverage area and all eight weather patterns (see section 2.1.1) in three steps:

(I) Trip fuel estimation

In a first step, the trip fuel is estimated assuming international standard atmosphere (ISA) conditions, a cruise flight with constant cruise mach number on flightlevel 340 and 5% contingency fuel.

For the original route network, each route is simulated as orthodrome (see section 2.2) from origin to destination. In contrast, for each surrogate route r, the trip fuel estimation is based on the adjusted ASK weighted mean orthodrome distance $\bar{d}_r$ of the associated original routes:

$$\bar{d}_r = \frac{\sum_{k=1}^{n_r} d_{\mathrm{Orth},r,k} \cdot \mathrm{ASK}_{\mathrm{adj},r,k}}{\sum_{k=1}^{n_r} \mathrm{ASK}_{\mathrm{adj},r,k}} \qquad (9)$$

(II) Fuel at final intersection point

Secondly, the amount of unburned fuel at the final intersection point with the CCF coverage area is calculated for all routes of both route networks. Following the approach from (I), an average rest distance $\bar{d}_{\mathrm{Rest},r}$ from the final intersection point to the destination is assumed for each surrogate route r based on the adjusted ASK weighted average orthodrome rest distance:

$$\bar{d}_{\mathrm{Rest},r} = \frac{\sum_{k=1}^{n_r} d_{\mathrm{Orth,Rest},r,k} \cdot \mathrm{ASK}_{\mathrm{adj},r,k}}{\sum_{k=1}^{n_r} \mathrm{ASK}_{\mathrm{adj},r,k}} \qquad (10)$$

(III) Final trajectory simulation

Finally, for each route, the climate impact caused within the CCF coverage area is calculated assuming a great circle connection. Wind, pressure and temperature distributions are considered individually for each weather pattern. The amount of remaining fuel at the final intersection point determined in (II) is defined as boundary condition in the trajectory simulations. Subsequently, the total climate impact caused within the CCF coverage area is estimated for both networks by summing up the climate impact contributions of all routes for all weather patterns w_i individually. The relative climate impact deviation $\Delta\mathrm{ATR}_{20,\mathrm{rel},w_i}$ between the original (index o) and the surrogate (index s) route network is estimated according to Eq. (11).

$$\Delta\mathrm{ATR}_{20,\mathrm{rel},w_i} = \frac{\mathrm{ATR}_{20,s,w_i} - \mathrm{ATR}_{20,o,w_i}}{\mathrm{ATR}_{20,o,w_i}} \qquad (11)$$

Based on the weather pattern frequencies f_{w_i} from Tab. 2, the weighted mean value of the climate impact deviation $\Delta\overline{\mathrm{ATR}}_{20,\mathrm{rel}}$ is obtained as illustrated in Eq. (12) and plotted in Fig. 5 for different network fractions n.

$$\Delta\overline{\mathrm{ATR}}_{20,\mathrm{rel}} = \frac{\sum_i f_{w_i}\mathrm{ATR}_{20,s,w_i} - \sum_i f_{w_i}\mathrm{ATR}_{20,o,w_i}}{\sum_i f_{w_i}\mathrm{ATR}_{20,o,w_i}} \qquad (12)$$

Tab. 2: Frequencies f_w (days/year) of the North Atlantic weather patterns [4].

	w_1	w_2	w_3	w_4	w_5	w_6	w_7	w_8
f_w	17	17	15	15	26	19	55	18

The resulting mean climate impact deviation $\Delta\overline{\mathrm{ATR}}_{20,\mathrm{rel}}$ (solid line) generally shows a decreasing tendency with increasing network fraction n and reduces from 7% for n = 6 to 2.5% for n = 10. However, $\Delta\overline{\mathrm{ATR}}_{20,\mathrm{rel}}$ is alternating since the vast majority of air traffic, which is intersecting the eastern bound of the CCF coverage area between 50° and 57° latitude (see Fig. 1), is allocated to one segment for even n (higher deviation) and two segments for odd n (lower deviation). Independent of n, the minimum and maximum climate impact deviations of single weather patterns (dashed lines), fluctuate about ±2% around the mean climate impact deviation.

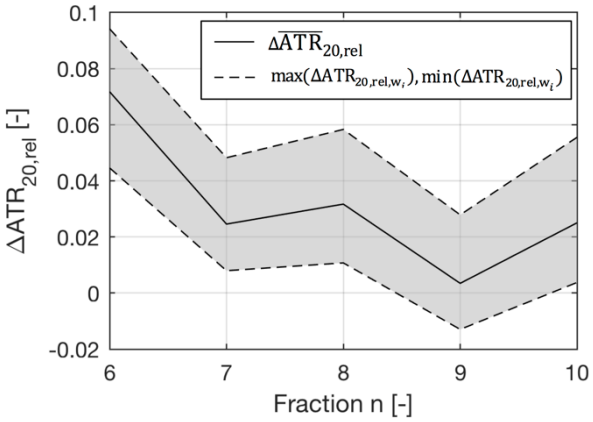

Fig. 5: Relative climate impact deviation between original and reduced North Atlantic route network as a function of the network fineness n.

To analyze a variety of different climate impact mitigation options, the simulation of 40 routes (3% of the original 1,359 routes) seems to be feasible in terms of computational resources and sufficient in terms of adjusted ASK for $n < 8$, as more than 90% of the adjusted ASK are covered (see Fig. 4). Thus, an odd network fraction of n = 7 is selected, which is characterized by a mean climate impact deviation of about 2.5%; a deviation much lower than existing uncertainties in climate impact prediction [17].

4 Optimization results

In the next section, climate and weather optimized trajectories are presented exemplarily for the top 1 westbound route from segment e to segment G of the previously selected surrogate route network (see Tab. 1; Fig. 3), which represents 13.6% of the adjusted ASK of the original route network. Results are discussed for a single weather situation on trajectory level first (see section 4.1). Then, consolidated results for all eight weather patterns are presented (see section 4.2).

4.1 Single weather situation

The following climate and weather optimized aircraft trajectories have been generated with TOM (see section 2) applying the cost functional

from section 2.1 and assuming free flight conditions. All simulations were performed with a BADA 4.2 Boeing 777-300ER aircraft performance model assuming a constant cruise Mach number of 0.84. The meteorological conditions as well as the CCFs were obtained from weather pattern w_1 at 12:00 p.m. UTC.

In Fig. 6, climate and weather optimized trajectories are depicted for the route e-G. Colors represent the magnitude of the wind speed (a) and the climate sensitivity (b). In order to avoid the jet stream, the minimum DOC trajectory (solid black trajectory; $c_\Psi = 0$) is located in the north of the orthodrome (blue line). While increasing the climate weighting factor c_Ψ (see Eq. (3)), the trajectories are shifted even more northwards to regions with lower climate sensitivities (see dashed and dash-dotted trajectories).

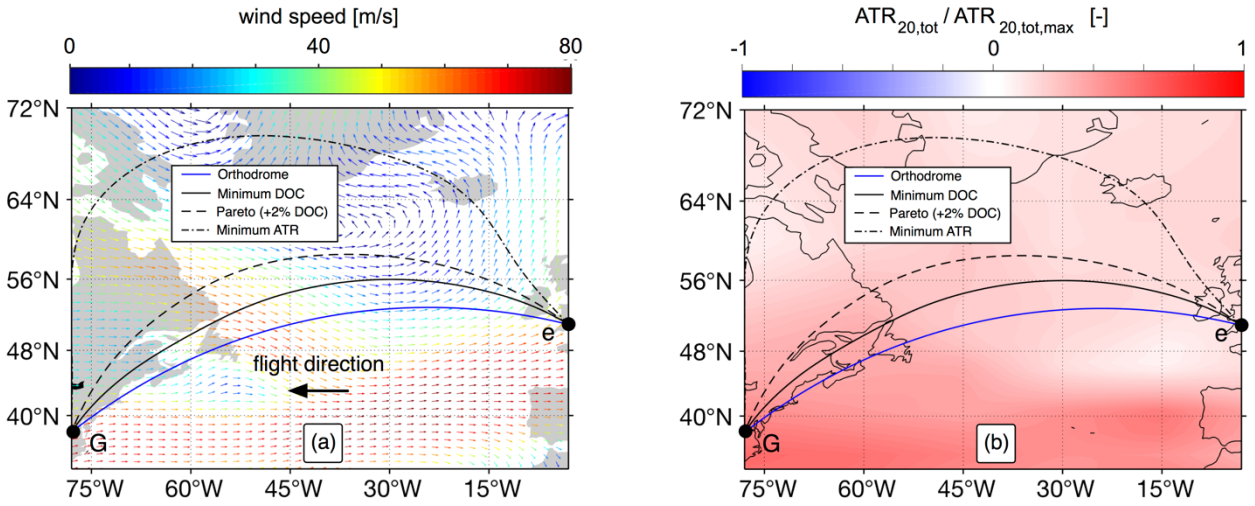

Fig. 6: Latitude-longitude plot of optimized trajectories on route e-G with varying climate weighting factors. Wind speeds and directions (a) and total climate cost (b) are shown for flight level 340.

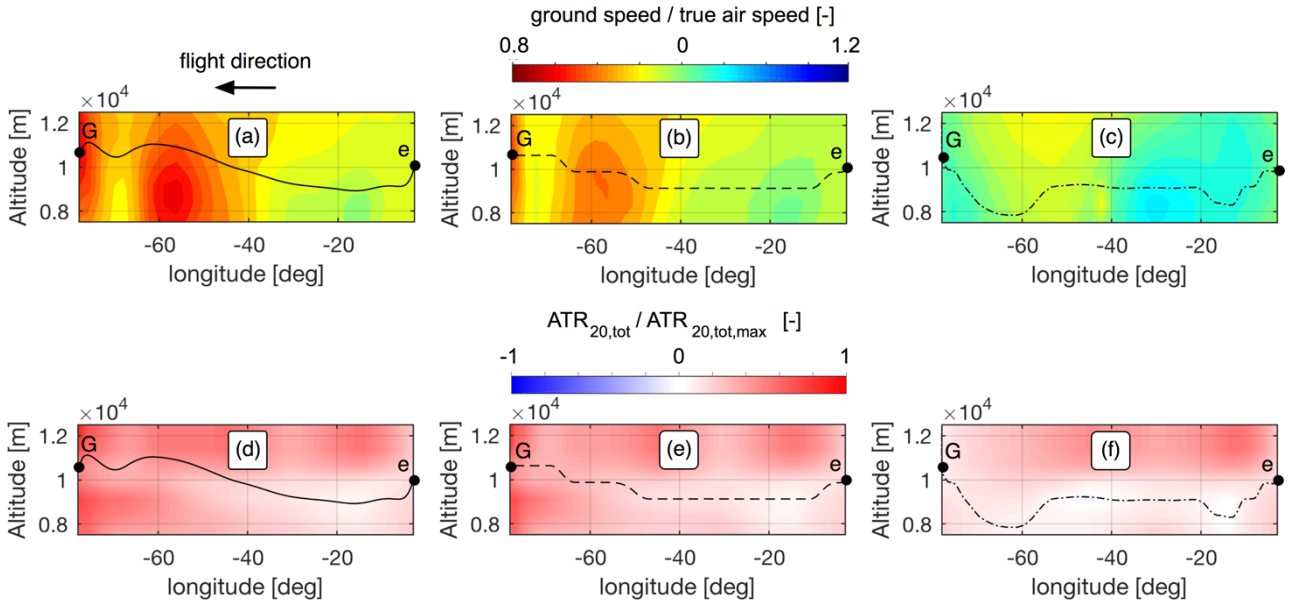

Fig. 7: Altitude-longitude plots of optimized trajectories on route e-G for varying climate weighting factors. Wind data (a-c) and total climate costs (d-f) are shown along the cross section of the lateral path. Figures represent minimum DOC (a,d), minimum ATR (c,f) and Pareto-optimal trajectories (b,e).

Vertical flight profiles are plotted in Fig. 7 for the minimum DOC (a,d), the +2% DOC Pareto-optimal (b,e), as well as the minimum ATR trajectory (c,f). The shape of the minimum DOC trajectory (a,d) is essentially driven by the avoidance of head winds[4] which especially occur in the second half of the flight. If the importance of climate impact reduction is increased (b-c, e-f), the influence of wind decreases and the vertical profiles are adjusted to regions with lower climate sensitivities.[5]

Pareto-optimal trajectories have been generated for a variety of climate weighting factors between 0 and 1 (see Eq. 2). The resulting Pareto front, illustrating the potential climate impact savings as a function of the DOC penalty is shown in Fig. 8. All results are expressed relative to the values of the minimum DOC trajectory (reference) according to Eq. (12) and (13), which also contain the individual contributions of each emissions species $i \in CO_2$, H_2O, NOx.

$$\Delta \mathrm{DOC}_{\mathrm{rel}} = \frac{\mathrm{DOC} - \mathrm{DOC}_{\mathrm{ref}}}{\mathrm{DOC}_{\mathrm{ref}}} \qquad (13)$$

$$\Delta \mathrm{ATR}_{20,\mathrm{rel},i} = \frac{\mathrm{ATR}_{20,i} - \mathrm{ATR}_{20,\mathrm{ref},i}}{\mathrm{ATR}_{20,\mathrm{ref,total}}} \qquad (13)$$

The Pareto front indicates a maximum total climate impact reduction potential (black dots) of almost 60% going along with a DOC penalty of about 16%. However, much higher total climate impact mitigation efficiencies (climate impact reduction per cost increase) are obtained at lower DOC penalties. E.g. at a cost penalty of 2%, a total climate impact reduction of 25% is observed.

As shown in Fig. 8, the total climate impact mitigation potential of this particular route and weather situation is essentially driven by reducing the climate impact caused by NO_x-emissions (red dots). $\Delta \mathrm{ATR}_{20,\mathrm{rel},NO_x}$ is overcompensating the additional climate impact caused by increased CO_2-emissions (grey dots) resulting from headwinds, detours as well as off-design altitudes.

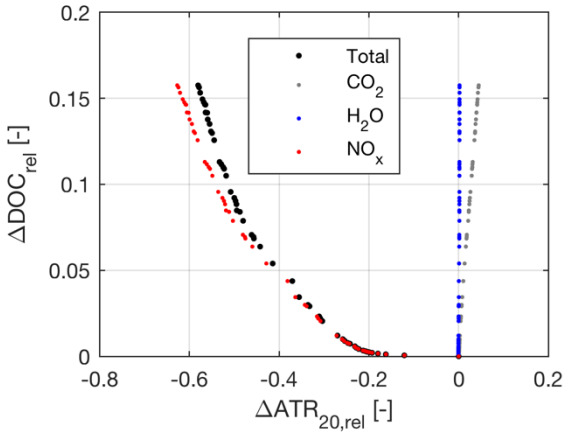

Fig. 8: Pareto front for weather pattern w_1 with the individual climate impact reduction contributions from CO_2, H_2O and NO_x. Results are normalized with respect to the minimum DOC trajectory.

4.2 Consolidated results

For all weather patterns, lateral flight profiles of minimum DOC trajectories and minimum climate impact trajectories for the route e-G are shown in Fig. 9. While the minimum DOC trajectories (a) only show latitudinal variations of about 10° between the different weather patterns, minimum climate impact trajectories (b) show much higher lateral deviations from each other.

Pareto fronts for the route e-G for all eight weather patterns are shown in Fig. 10 (grey markers). The maximum climate impact reduction potential scatters significantly for varying weather patterns; values range between 9% (w_6) and 60% (w_5). Also, climate impact mitigation efficiencies differ strongly: e.g. for a DOC penalty of 2%, total climate impact reductions between 9% (w_6) and 44% (w_5) are observed.

To determine an average Pareto front, which considers the annual frequencies of the weather patterns (see Tab. 2), individual Pareto fronts are combined optimally according to Eq. (14):

$$\min \sum_i f_{w_i} \cdot \mathrm{ATR}_{20,w_i} \quad \text{subject to} \quad \sum_i f_{w_i} \cdot \mathrm{DOC}_{w_i} < \mathrm{DOC}_{\mathrm{penalty}} \qquad (14)$$

[4] In (a-c) the direction of the wind is expressed as the ratio of ground speed and true air speed (headwinds: ratio < 1, tailwinds: ratio > 1)

[5] A more detailed analysis on trajectory level for a similar route is given by Lührs et al. (2016) [6].

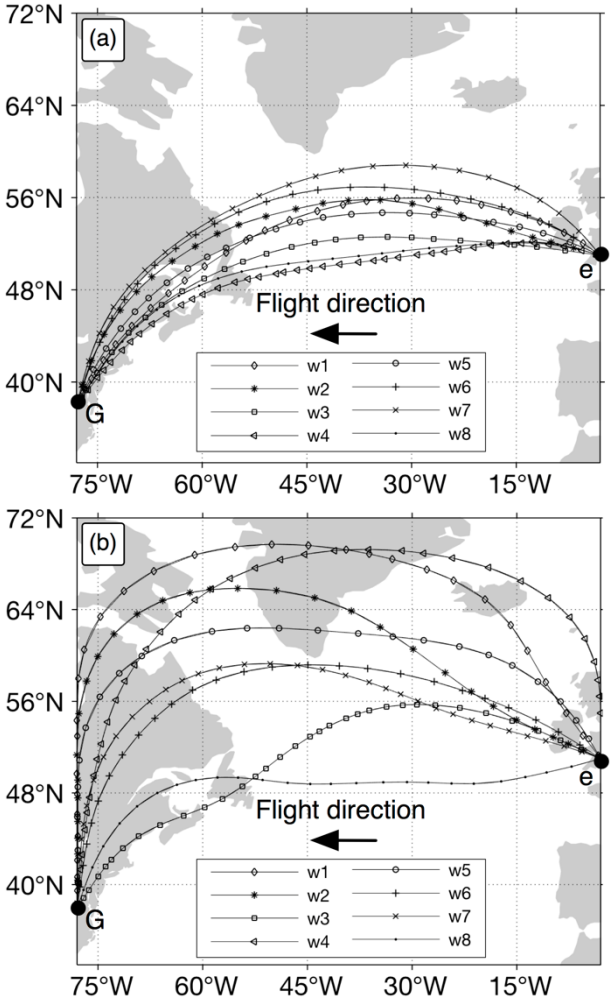

Fig. 9: Latitude - longitude plots of minimum DOC trajectories (a) and minimum climate impact trajectories (b) for all weather patterns.

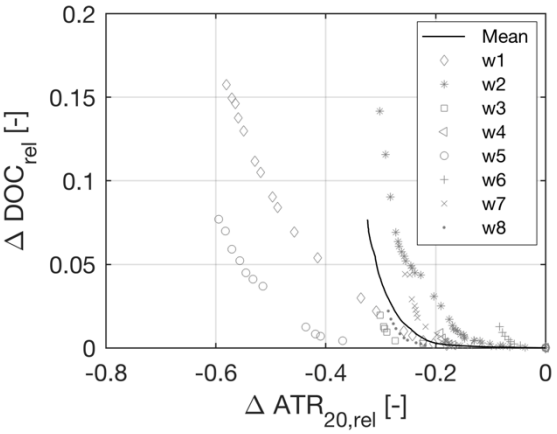

Fig. 10: Pareto fronts (total) for all weather patterns (grey markers) and averaged Pareto front (black line) for the westbound route e-G.

This problem is reformulated in MATLAB as integer linear programming problem and solved for various DOC penalties. The resulting mean Pareto front indicates a maximum climate impact reduction potential of 32.4% at a DOC penalty of 7.7% (see Fig. 10, black line). However, 24% climate impact reduction can already be achieved for 1% additional DOC.

Since any deviation from the cost optimal trajectory is related with increased DOC, climate impact mitigation does not coincide with cost reduction. To create a financial incentive for airlines to minimize flight time and emissions in highly climate sensitive regions, Niklaß et al. (2018) suggest levying a climate charge for transition. Thus, cost-minimizing airlines will re-route their flights voluntarily to reduce the sum of both, climate charges and direct operating costs [18].

5 Conclusion and outlook

To reduce the computational effort for aircraft trajectory calculations and associated climate impact estimations, a method for the generation of reduced surrogate route networks in the North Atlantic flight corridor has been proposed. For the scheduled North Atlantic air traffic of the year 2016, the applied simplification allows for a reduction from 1,359 to 40 routes while covering more than 90% of the available seat kilometers (ASK).

Using the surrogate network, the climate impact of the original route network can be reproduced with reasonable mean climate impact deviations of about 2.5% for CO_2, H_2O and NO_x. However, the comparison has only been evaluated for one specific altitude and since climate impact strongly depends on altitude, a sensitivity analysis is required in future studies. Additionally, the proposed methodology needs to be verified for the reproduction of the climate impact caused by contrail induced cirrus cloudiness which is characterized by strong lateral and vertical gradients and hence may increase the climate impact deviations resulting from the network simplification.

In the second part of the study, a cost-benefit analysis has been performed for the top 1 route of the surrogate route network trading-off climate impact reduction vs. rise of direct operating costs. Maximum climate impact savings have been found to differ significantly

between individual weather patterns and range from 9% to 60%. Averaged over the weather patterns, potential climate impact savings of about 24% have been observed for a 1% cost penalty. Maximum climate impact savings of approximately 32% can be reached for a cost penalty of about 8%. However, this potential is based on the assumption of free flight conditions and hence may not be fully achieved due to air traffic regulations. Thus, the integration of air traffic constraints is planned for future investigations. Additionally, the cost-benefit analysis performed in this study will be extended to consider all routes of the surrogate route network.

Acknowledgements

The weather based climate change functions were derived within the EU-project REACT4C, funded under the EU 7th framework program, grant ACP8-GA-2009-233772. Further, we thank EUROCONTROL for providing BADA 4.2 aircraft performance data.

References

[1] Airbus: Global Market Forecast: *Flying by Numbers 2017 - 2036*. Blagnac, FRA, April 2017. ISBN-13: 978-2-9554382-2-6.

[2] IATA: *Technology Roadmap of the International Air Transport Association*. Ed. 4. Montreal, CAN, June 2013.

[3] IPCC: Climate Change 2013 - the Physical Science Basis. *Contribution of Working Group I to the Fifth Assessment Report of the Intergovernmental Panel on Climate Change*. Cambridge University Press, Cambridge, UK, 2013. ISBN-13: 978-1-107-05799-1

[4] Frömming, C.; Grewe, V.; Jöckel, P.: *Climate cost functions as a basis for climate optimized flight trajectories*, ATM Res. Dev. Seminar, 10, 2013.

[5] Grewe et al.: *Aircraft routing with minimal climate impact: The REACT4C climate cost function modelling approach (V1.0)*. Geosci. Model Dev., 7, 175-201, 2014. doi: 10.5194/gmd-7-175-2014.

[6] Lührs, B.; Niklaß, M; Frömming, C.; Grewe, V.; Gollnick, V.: *Cost-Benefit Assessment of 2D- and 3D Climate and Weather Optimized Trajectories*. 16th ATIO conference, 2016.

[7] Nuic, A.; Mouillet, V.: *User Manual for the Base of Aircraft Data (BADA) Family 4*. ECC Technical/Scientific Report No. 12/11/22-58, 2012.

[8] Jelinek et al.: *Advanced Emission Model (AEM3) v1.5 - Validation Report*. EEC Report EEC/SEE/2004/004, 2004.

[9] DuBois, D.; Paynter, G.: *'Fuel Flow Method 2' for Estimating Aircraft Emissions*. Society of Automotive Engineers (SAE), SAE Technical Paper 2006-01-1987, 2006.

[10] Patterson, M.A.; Rao, A.V.: *GPOPS-II: A MATLAB Software for Solving Multiple-Phase Optimal Control Problems Using hp-Adaptive Gaussian Quadrature Collocation Methods and Sparse Nonlinear Programming*. ACM Transactions on Mathematical Software, Vol. 1, No. 1, Article 1, 2014.

[11] Wächter, A.; Biegler, L. T.: *On the implementation of an interior-point filter line-search algorithm for large-scale nonlinear programming*. Mathematical Programming. Vol. 106, pp. 25-57, 2006.

[12] Jöckel, P.; Kerkweg, A., Pozzer, A. Sander, R.; Tost, H., Riede, H., Baumgaertner, A., Gromov, S., Kern B., *Development cycle 2 of the modular earth submodel system (MESSy2)*. Geosci. Model Dev. 2010, 3. 717-752. Doi:10.5194/gmd-3-717-2010.

[13] Irvine, E. A.; Hoskins, B. J.; Shine, K. P.; Lunnon, R. W.; Frömming, C.: *Characterizing north Atlantic weather patterns for climate-optimal routing*. Meteorol. Appl. 20, 80-93, 2013.

[14] Thorbeck, J.*: TU Berlin DOC Method as proposed in lecture notes „Flugzeugentwurf“,* 2012.

[15] International Monetary Fund*, World Economic Outlook Database,* April 2018.

[16] Airport Data Intelligence (ADI), Sabre Airline Solutions, Southlake, TX, 2018, https://www.sabreairlinesolutions.com/home/software_solutions/airports [retrieved 26 February 2018].

[17] Grewe et al.: Mitigating the Climate Impact from Aviation. Achievements and Results of the DLR WeCare Project. *Aerospace* 2017, 4, 34; doi:10.3390/aerospace4030034

[18] Niklaß, M.; Lührs, B.; Grewe, V.; Gollnick. V.: *Implementation of eco-efficient procedures to mitigate the climate impact of non-CO_2 effects*. 31st ICAS congress, Brazil, 2018.

Copyright Statement

Contact Author Email Address

benjamin.luehrs@tuhh.de